

FROM GEO/LEO ENVIRONMENT DATA TO THE NUMERICAL ESTIMATION OF SPACECRAFT SURFACE CHARGING AT MEO

Jean-Charles Matéo-Vélez⁽¹⁾, Nataly Ganushkina⁽²⁾, Nigel Meredith⁽³⁾, Angélica Sicard-Piet⁽¹⁾, Vincent Maget⁽¹⁾, Denis Payan⁽⁴⁾, I. Sillanpaa⁽²⁾, S. Dubyagin⁽²⁾

⁽¹⁾ONERA, The French Aerospace Lab, 2 avenue Edouard Belin, 31055 Toulouse, France
jean-charles.mateo_vez@onera.fr

⁽²⁾Finnish Meteorological Institute, P.O. BOX 503, FI-00101 Helsinki, Finland
Nataly.Ganushkina@fmi.fi

⁽³⁾British Antarctic Survey, High Cross, Madingley Road, Cambridge, UK
nmer@bas.ac.uk

ABSTRACT

This paper aims at defining a series of severe plasma environments in terms of spacecraft surface charging in middle Earth orbit especially for the Global Navigation Satellite System. As few low energy plasma monitors are flying in this region of the radiation belts, measurements done at geostationary orbit are extrapolated by numerical simulation. Three criteria are used to select the electron spectra: large spacecraft absolute potential, high electron fluxes at all energies, and high electron fluxes except at high energy. In this paper, we will present a physical model to extrapolate these severe environments measured in GEO to MEO using the Inner Magnetosphere Particle Transport and Acceleration model program. In addition, we analyze the 30 keV electron measurements of the POES satellite in LEO to provide a qualitative countermeasure at L* of 6 and 4.5.

1. INTRODUCTION

Spacecraft charging is impacted by electrons and protons of low to medium energy, typically in the range between a few keV to some hundreds of keV. Assessing charging levels by numerical simulation becomes possible through the availability of more and more software tools and their cross-comparison. This was especially done under GEO worst-case environments ([1], [2], [3], [4]) known to be responsible for spacecraft power losses. This approach depends on our ability to predict the ambient plasma conditions encountered in orbit. In recent decades, many instruments have been flown and have measured low energy electron and proton distributions (GOES, POES, CRRES, CLUSTER, etc...) but only a few of them cross the MEO orbit and the Global Positioning System data are not publicly available. A recent paper dealing with Van Allen Probe potential measurements showed that strong negative charging occurred primarily at high Ls in the post-midnight sector [5]. This strong negative charging (some hundreds of volts) above $L > 3$ occurred while the spacecraft was not in eclipse which is surprising

since the RBSP spacecraft is totally conductive. Even if the charging levels are lower than non-conducting spacecraft at GEO (SCATHA suffered a -8 kV in 1979) one can conclude that conductive spacecraft are able to charge negative under certain conditions. A few other plasma measurements are available at MEO on Themis but globally, this area is much more unknown than GEO and LEO in terms of low energy particle fluxes.

This paper presents a complementary approach consisting in modelling the low energy population dynamics inside the radiation belts, using GEO spacecraft measurements as input and LEO instruments as additional information for results analysis. In section 2, we discuss the method used to obtain the spacecraft potential from the flight data in GEO. In section 3, we select one severe environment that was measured in GEO on January 02, 2005 and analyse corresponding LEO observations. Section 4 describes the simulation of the low energy electron dynamics within the radiation belts during that day, especially at MEO.

2. SELECTION OF SEVERE GEO ENVIRONMENTS

Several worst-case environments have been proposed for GEO surface charging ([1]-[4]). In this work we focus on some of them, extracted from [4] and obtained from the Los Alamos National Laboratory (LANL) spacecraft equipped with electron detectors between 1keV and a few MeV as well as low energy ion detectors used to estimate the spacecraft negative potential.

The spacecraft potential is a mean to assess the risk associated to electron and proton spectra. It however distorts the distribution functions so measurements need some corrections. The spacecraft potential is obtained with the electron saturation flux at low energies when the spacecraft is positive (recollection of photoelectrons and/or secondary electrons). When the spacecraft is negative, which is the most dangerous situation considered in this paper, the proton peak flux energy

can be used, as done for instance in [5]. LANL data are post processed following a different approach because the proton peak is not always visible, probably due to pollution of low energy channels by energetic particles during large events or less probably by secondary electrons. The method described in [6]-[7] assumes an empirical and analytical relation between the absolute spacecraft potential and the moments of the distribution functions. The two methods generally agree. Discrepancies however occur when dealing with some charging events, see Fig.1 where large potentials can be given by a method and not by the other. This kind of differences is always observed when using two different instruments for measuring the same quantity [5] or when two methods are used to extract the same information from a dataset. This is visible on the top 100 environments associated to the highest flux at all energies (HFAE) criterion, where potentials of -10 kV are exceeded with the moment method while the proton peak gives a maximum of -3 kV. The top 100 environments associated to the low flux at high energies (LFHE) and high flux at low energy criterion exhibits also a large dispersion. Several potentials are underestimated by the moments method, but globally it tends to overestimate the results by a factor of 2 with respect to the ion peak method.

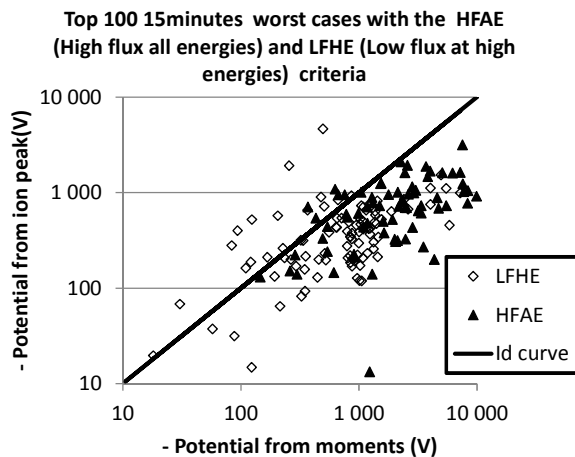


Figure 1. Potentials during the top 100 worst environments following the HFAE and LFHE criteria

The difference is also visible with the top 100 events associated with negative potentials given by: 1/ the moment method and larger in absolute values than -2 kV, -5 kV and -10 kV: 2/ the ion peak method and larger in absolute values than -2 kV, -5 kV and -8 kV. The peak method does not provide potentials exceeding -8.5 kV. Both methods agree quite well below 8 kV negative, see Fig. 2.

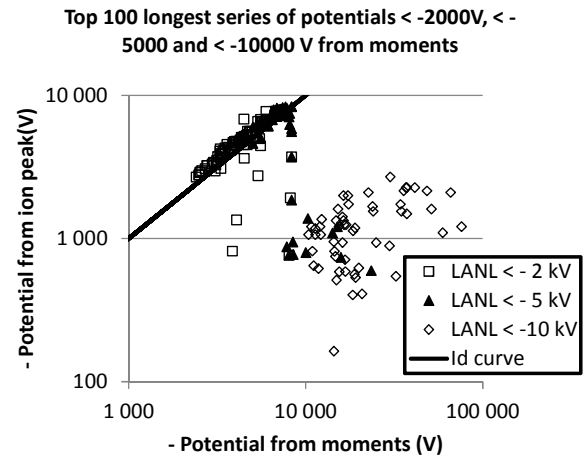


Figure 2. Potentials during the top 100 worst environments associated to large potentials given by the moment method

For the rest of the paper we will focus on a severe GEO environment measured on LANL_1994_084 on 2005/01/02 at 15h46min12s UTC time and at MLT of 04 47. The average potential during 15 minutes around that date was estimated between -650 Volts and -3200 Volts pending on the method used. This absolute charging was associated to a large integral electron flux of $5 \times 10^8 \text{ cm}^{-2} \cdot \text{s}^{-1} \cdot \text{sr}^{-1}$ (HFAE criterion).

3. CORRELATION WITH LEO OBSERVATIONS

This section is based on the analysis of extreme energetic electron fluxes in LEO performed on NOAA-15_to_19 POES spacecraft [8]. We have focused on the electrons of energy above 30 keV at L^* of 6.0 and 4.5 on January 02, 2005, see Fig. 3. The data plotted correspond to the maximal 2s fluxes each 3 hours. It is compared to the average flux at a given L^* and to the 5%, 1% and 0.1% exceedance flux level which also are functions of L^* . At $L^* = 6.0$, the flux around 16h00 UTC time exceeds slightly the 5% exc. level. It was preceded by three events of same intensity on the same or previous day, confirming the large electron fluxes measured by LANL. The fluxes at $L^*=4.5$ have approximately the same value as $L^*=6.0$ but it is worth noticing that this flux exceeds strongly the local 5% exc. level and are very close to the 1% exc. level.

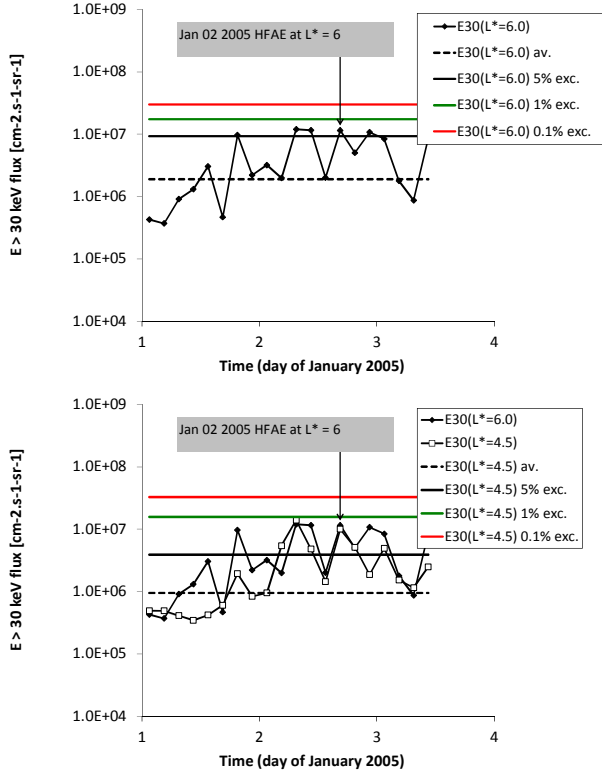


Figure 3. $E > 30$ keV electron fluxes at LEO and $L^* = 6.0$ (top) and $L^* = 4.5$ (bottom)

4. MEO ENVIRONMENT MODELLING

The Inner Magnetosphere Particle Transport and Acceleration model (IMPTAM) traces distributions of electrons in the drift approximation (1st and 2nd adiabatic invariants conserved) with arbitrary pitch angles from the plasma sheet (starting from $L=10$) to the inner L shell regions with energies reaching up to hundreds of keVs in time-dependent magnetic and electric fields [9]-[10]-[11]. We obtain the changes in the electron

distribution function $f(R, \phi, t, E_{kin}, \alpha)$, where R and ϕ

are the radial and azimuthal coordinates in the equatorial plane, respectively, t is the time, E_{kin} is the

particle energy, and α is the particle pitch angle,

considering the drift velocity as a combination of the $\mathbf{E} \times \mathbf{B}$ drift velocity and the velocities of gradient and curvature drifts. Liouville's theorem is used to gain information of the entire distribution function with losses taken into account. For the obtained distribution function, we apply radial diffusion by solving the radial diffusion equation the distribution function. Kp -

dependent radial diffusion coefficients D_{LL} for the magnetic field fluctuations are computed following [12] using $D_{LL} = 10^{0.056Kp-9.325} L^{10}$. After that, we repeat the order of calculation: first, we solve transport with losses and then apply the diffusion. For electron losses we consider convection outflow and pitch angle diffusion by introducing the electron lifetimes according to *Chen et al.* [2005] for the strong diffusion and [13] for the weak diffusion regimes.

For calculations at MEO, we use the set of models which was found to provide best agreement with the measured low-energy electron fluxes at geostationary orbit: (1) a dipole model for the internal magnetic field, (2) T96 model [14] for the external magnetic field with Dst , Psw , IMF B_y and B_z as input parameters, and (3) [15] polar cap potential dependent on solar wind and IMF parameters mapped to the magnetosphere.

We set the model boundary at $10 RE$ and use the kappa electron distribution function with kappa of 1.8. The number density n and temperature T in the distribution function are given by the empirical model derived from Geotail data by [16]. The electron n is assumed to be the same as that for ions in the model, but $Te/Ti = 0.2$ is taken into account. We also introduced a time shift of 2 h following [17] for the solar wind material to reach the midtail plasma sheet.

LANL data are used as input for IMPTAM every 5 minutes. Fig. 5 shows a good agreement between the LANL data and the environment computed with IMPTAM at GEO below 100 keV, which is the upper boundary of the computational program. A large increase in the fluxes is obtained at MEO, up to a factor of 10 at energies below 15 keV and up to a factor of 50 above 35 keV.

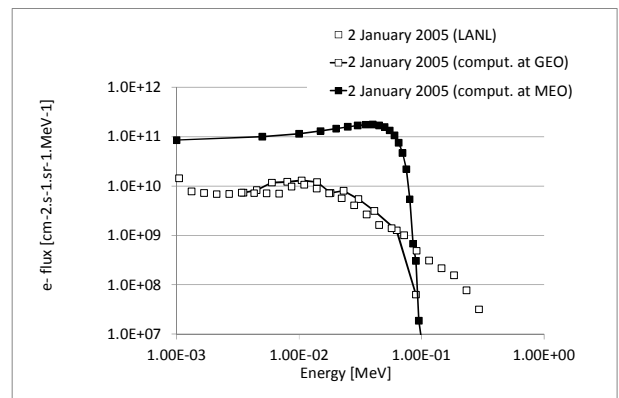


Figure 5. Comparison of LANL and IMPTAM fluxes at GEO and flux computed at MEO

5. CONCLUSION

This paper presented a method to correlate plasma measurements made at GEO and at LEO with simulations of the low energy electron dynamics inside

the radiation belts. POES and LANL data have been used at LEO and GEO respectively during the event that occurred on LANL spacecraft on January 02, 2005. The IMPTAM program provided detailed description of low energy electron transport from GEO to MEO, indicating that fluxes tends to increase significantly. The next steps will consist in analyzing other events and determine how to improve the precision of the method, especially by inspecting E>100 keV electrons. The impact on MEO spacecraft charging will be assessed by analytical and numerical estimations and conclusion drawn for electrostatic discharges risk assessment at MEO with respect to GEO.

6. ACKNOWLEDGEMENTS

This work was partly funded by CNES R&D program and partly by the European Union Seventh Framework Programme (FP7/2007-2013) under grant agreement no 606716 (Spacestorm).

7. REFERENCES

1. Ferguson, D. C., and Wimberly, S. C., "The Best GEO Daytime Spacecraft Charging Index," 51st AIAA Aerospace Sciences Meeting including the New Horizons Forum and Aerospace Exposition, AIAA, Grapevine, TX, 2013.
2. Toyoda, K., and Ferguson, D. C., "Round-Robin Simulation for GEO Worst-Case Environment for Spacecraft Charging," 13th Spacecraft Charging and Technology Conference, Pasadena, CL, 2014.
3. Ferguson, D. C., Hilmer, R. V., Wheelock, A. T., & Davis, V. A., "The Best GEO Daytime Spacecraft Charging Index – Part II," 52nd AIAA Aerospace Sciences Meeting, AIAA, National Harbor, MD, 2014.
4. J.C. Matéo-Vélez et al., "Severe geostationary environments: numerical estimation of spacecraft surface charging from flight data", to be published in *J. Spacecraft and Rockets*, 2016.
5. L. K. Sarno-Smith et al., "Spacecraft Surface Charging within Geosynchronous Orbit Observed by the Van Allen Probes", accepted in *American Geophysical Union*, 2016.
6. Thomsen, M., et al., "Calculation of moments from measurements by the Los Alamos Magnetosphere Plasma Analyzer," LANL Report, LA-13566-MS, 1999.
7. Davis, V. A., Mandell, M. J. and Thomsen, M., "Representation of the measured geosynchronous plasma environment in spacecraft charging calculations," *J. Geophys. Res.*, 113, A10204, 2008. doi:10.1029/2008JA013116.
8. Meredith, N. P., R. B. Horne, J. D. Isles, and J. C. Green (2016), "Extreme energetic electron fluxes in low Earth orbit: Analysis of POES E>30, E>100, and E>300 keV electrons", *Space Weather*, 14, 136–150, doi:10.1002/2015SW001348
9. Ganushkina, N. Y., O. A. Amariutei, D. Welling, and D. Heynderickx, (2015), Nowcast model for low-energy electrons in the inner magnetosphere, *Space Weather*, 13, doi:10.1002/2014SW001098.
10. Ganushkina N. Yu., M. Liemohn, O. Amariutei, and D. Pitchford (2014), Low energy electrons (5-50 keV) in the inner magnetosphere, *J. Geophys. Res.*, 119, doi:10.1002/2013JA019304
11. Ganushkina, N. Y., O. A. Amariutei, Y. Y. Shprits, and M. W. Liemohn (2013), Transport of the plasma sheet electrons to the geostationary distances, *J. Geophys. Res.: Space Physics*, 118, doi:10.1029/2012JA017923.
12. Brautigam, D. H., and J. M. Albert (2000), Radial diffusion analysis of outer radiation belt electrons during the October 9, 1990, magnetic storm, *J. Geophys. Res.*, 105(A1), 291–309, doi:10.1029/1999JA900344.
13. Shprits, Y. Y., N. P. Meredith, and R. M. Thorne (2007), Parameterization of radiation belt electron loss timescales due to interactions with chorus waves, *Geophys. Res. Lett.*, 34, L11110, doi:10.1029/2006GL029050.
14. Tsyganenko, N. A. (1995), Modeling the Earth's magnetospheric magnetic field confined within a realistic magnetopause, *J. Geophys. Res.*, 100(A4), 5599–5612, doi:10.1029/94JA03193.
15. Boyle, C. B., Reiff, P. H., & Hairston, M. R. (1997). Empirical polar cap potentials. *Journal of Geophysical Research*, 102(A1), 111-125.
16. Tsyganenko, N. A., and T. Mukai (2003), Tail plasma sheet models derived from Geotail particle data, *J. Geophys. Res.*, 108, 1136, doi:10.1029/2002JA009707, A3.
17. Borovsky, J. E., Thomsen, M. F., & Elphic, R. C. (1998). The driving of the plasma sheet by the solar wind. *Journal of Geophysical Research: Space Physics*, 103(A8), 17617-17639.